

NASA TECHNICAL TRANSLATION

NASA TT F-16902

CALCULATION OF MUSCULAR POWER IN FLAPPING FLIGHT  
OF BIRDS FROM KINEMATIC AND MORPHOLOGICAL DATA  
(STUDIES ON BIOPHYSICS AND PHYSIOLOGY OF AVIAN  
FLIGHT III)

H. Oehme and U. Kitzler

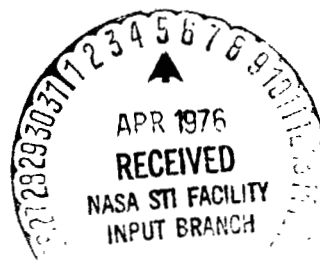
(NASA-TT-F-16902) CALCULATION OF MUSCULAR  
POWER IN FLAPPING FLIGHT OF BIRDS FROM  
KINEMATIC AND MORPHOLOGICAL DATA (STUDIES ON  
BIOPHYSICS AND PHYSIOLOGY OF AVIAN FLIGHT 3)  
(Kanner (Leo) Associates) 54 p HC \$4.50

N76-20796

Unclas  
20746

G3/51

Translation of "Die Bestimmung der Muskelleistung  
beim Kraftflug der Vogel aus kinematischen  
und morphologischen Daten (Untersuchungen zur  
Flugbiophysik und Flugphysiologie der Vogel III)  
Zoologische jahrbucher. Abteilung fur allgemeine  
zoologie und physiologie der tiere, Vol. 79, No. 3,  
1975, pp 425-458



## STANDARD TITLE PAGE

1. Report No. NASA TT F-16902	2. Government Accession No.	3. Recipient's Catalog No.	
4. Title and Subtitle CALCULATION OF MUSCULAR POWER IN FLAP- PING FLIGHT OF BIRDS FROM KINEMATIC AND MORPHOLOGICAL DATA (STUDIES ON BIOPHYSICS AND PHYSIOLOGY OF AVIAN FLIGHT III)		5. Report Date March 1976	6. Performing Organization Code
		8. Performing Organization Report No.	10. Work Unit No.
9. Performing Organization Name and Address Leo Kanner Associates, Redwood City, California 94063		11. Contract or Grant No. NASW-2790	13. Type of Report and Period Covered Translation
12. Sponsoring Agency Name and Address National Aeronautics and Space Adminis- tration, Washington, D.C. 20546		14. Sponsoring Agency Code	
15. Supplementary Notes Translation of.. "Die Bestimmung der Muskelleistung beim Kraftflug der Vogel aus kinematischen und morphologischen Daten (Untersuchungen zur Flugbiophysik und Flugphysiologie der Vogel III)." Zoologische jahrbucher. Abteilung fur allgemeine zoologie und physiologie der tiere, Vol. 79, No. 3, 1975, pp 425-458.			
16. Abstract An airscrew-type calculation is employed to determine the power output of birds' pectoral muscles in level flight, without recourse to aerodynamic force coefficient. Down- stroke power is derived from required lift, point of application of tangential force along wing, and angular velocity. Kinematic data (duration of downstroke, duration of accelerated rotation at start of downstroke, and duration of total cycle, flight speed, stroke angle, stroke angle bisector) are obtained from films. Sample flights of pigeons and doves are analyzed, and compared with metabolic- physiological results, confirming the usability of this method. In both species, the power output per unit weight of the pectoral muscles (0.26-0.60 HP/kg) under prolonged load is 10 to 20 times that of mammalian muscles, except, probably, for the flight muscles of bats.			
17. Key Words (Selected by Author(s))		18. Distribution Statement  Unclassified-Unlimited	
19. Security Classif. (of this report) Unclassified	20. Security Classif. (of this page) Unclassified	21. No. of Pages	22. Price

## TABLE OF CONTENTS

Introduction	1
Part I:	
Calculation Procedure	2
List of Symbols	2
Forces During Stroke Cycle	5
Steady-state Rotating Propeller as Model for Wing	
Downstroke	6
Glauert's (1935) Principle of Airscrew Calculation and	
its Modification	8
Location of Effective Radius	16
Converting Average Downstroke Lift to Tangential Force	20
Effect of Initial Acceleration in Downstroke on Location	
of Effective radius	25
Execution of Power calculation -- Discussion of Method	25
Part II:	
Specific Power Capacity of Pectoral Muscles of Columbia	
livia (pigeon) and Streptopelia decaocto in Horizontal	
Flight	36
Material	36
Results and Discussion	38
Summary	47
References	49

CALCULATION OF MUSCULAR POWER IN FLAPPING FLIGHT OF BIRDS  
FROM KINEMATIC AND MORPHOLOGICAL DATA

H. Oehme and U. Kitzler  
Vertebrate Research Center of East German  
Academy of Sciences (in Berlin Zoo)

Introduction

The muscular power generated by a bird during flapping flight is a problem which has been discussed many times. If, like Brown (1961 a, b), one starts from the position that the power output of flight muscles, in particular that of the musculus pectoralis, is no larger than that of mammalian muscles, further analysis of flight compels one to assume that the flying bird has virtually ideal aerodynamic properties. This is because experimentally determined continuous and peak powers of mammalian muscles (see Henderson and Haggard 1925; Dickinson 1928; Brody 1945) are not large enough to supply the energy required during a wing stroke, even assuming the most favorable possible flow-mechanical conditions. Power outputs per unit weight of flight musculature in the range 0.6-3.8 HP/kg are known from various insect species (Nachtigall 1968), and even calculations of the "motor power" of a flapping bird employing certain aerodynamic assumptions (Oehme 1963, 1965; Pennycuik 1968 b; Oehme 1968 a, 1970 b) yielded specific muscular powers which far exceeded the "mammalian norm" (0.03-0.05 HP/kg). It is true that there were large individual variations in these results. Nevertheless, metabolic studies on flying birds (Pearson 1950, 1953; Lasiewski 1963; Pearson 1964; LeFebvre 1964; Tucker 1968 a and b, 1969) established, despite some

---

\*Numbers in the margin indicate pagination in the foreign text.

conflicting results, that the power output of the avian pectoralis must be substantially higher than that of mammalian muscles. So far, such findings have been obtained with very few species (hummingbird, pigeon, parakeet, sea gull). If the "motor power" of birds in free flight can be determined by other methods, this will be an important advance and may make it possible to make comparisons relatively soon between various species.

Complete computation of avian flight on aerodynamic principles requires a large number of parameters which can only be estimated or must simply be assumed, since they are different if not impossible to determine in a flying bird. In the sequel, we will present a possible method for calculating flight power which requires 427 relatively few and relatively readily measurable kinematic and morphological parameters. We will show how many of the initial values necessary in a strict aerodynamic treatment can be eliminated. The procedure is limited to unaccelerated horizontal flight. Special forms of flapping flight such as hovering, acceleration, and braking are not included. Nevertheless, the prolonged effort of horizontal and accelerated flight seems quite suitable for characterizing the energy consumed by the local motor apparatus of a flying animal.

The procedure will be developed and discussed in the first part of the work, and the results obtained by applying it to two species will be presented in the second part.

## Part I: Calculation Procedure

### List of Symbols

Symbol	Meaning
R	Length of extended wing from shoulder joint to wing tip = radius of screw circle of propeller
r	Distance along R of the wing element from axis of rotation

Symbol	Meaning
$r_K$	Distance of body contour of bird [from axis of rotation]
$r_z$	Distance of point of application of total circumferential force, effective radius
$r/R$	Radio coordinate
$l$	Chord depth of wing element = chord depth at $r$
$l/R$	Relative chord depth
$\phi$	Angle of advance of wing element $\phi = \arctan v (1 + a)/[\omega r(1 - b)]$
$\phi$	Wing angle, angle between $R$ and horizontal
$\phi_b$	Wing angle at conclusion of angular acceleration of downstroke
$\phi_0, \phi_u$	Upper and lower limits of stroke angle
$\delta \quad 0.5$	Angle of asymmetry of stroke angle
$(\phi_0 + \phi_u)$	
$t$	Time
$t_{ab}$	Duration of downstroke
$t_b$	Duration of accelerated downstroke
$t_{ges}$	Duration of stroke cycle
$\bar{H}_{ab}, \bar{H}_{auf}$	Average lift during downstroke and upstroke respectively
$H^* = U^* \cos \phi$	Relative stroke
$M$	Torque
$P$	Power
$\overline{P}_{ab}$	Average power of pair of wings during downstroke
$P^* = c_m/\lambda^3$	Relative power
$\rho$	Density of air
$c_a$	Lift or normal force coefficient
$c_{wp}$	Profile drag coefficient
$\epsilon_p = c_{wp}/c_a$	Profile drag-life ratio
$c_s$	Thrust coefficient of wing element
$c_u$	Circumferential force coefficient of wing element

Symbol	Meaning
$C_s$	Thrust coefficient of air screw or of wing pair
$C_u$	Circumferential force coefficient of air screw or wing pair
$C_m$	Torque coefficient of air screw or wing pair
$m$	Number of air screw blades <span style="float: right;">/428</span>
$\sigma = ml/(2\pi r)$	Percentage of circumference covered by wing element
$\lambda = v/(\omega R)$	Coefficient of advance
$\lambda_{\min} = v/(\omega_{\max} R)$	Smallest advance coefficient attained during downstroke
$\bar{\lambda}$	Average advance coefficient during downstroke
$k = \bar{U}/\bar{H}_{ab}$	Conversion factor for mean downstroke into mean circumferential force during downstroke
$\tau = t/t_{ab}$	Relative duration, normalized by duration of downstroke
$n = t_{ab}/t_b - 1$	Time factor of duration of acceleration during downstroke
$v$	Flight velocity
$w$	Effective relative air speed of a wing element
$\omega$	Angular velocity
$\omega_{\max}$	Largest angular velocity from initial acceleration of rotary motion of downstroke to end of downstroke
$\bar{\omega}$	Mean angular velocity of downstroke
$\alpha = \omega_{\max}/t_b$	Angular acceleration of downstroke
$a$	Coefficient for induced axial velocity
$b$	Coefficient for induced tangential velocity
$G$	Total weight
$G_{\text{Pect}}$	Weight of the two pectoral muscles
$A$	Lift or normal force
$W$	Drag
$S$	Thrust
$U$	Circumferential or tangential force
$U_{\max}$	Tangential force at $\omega_{\max}$

Symbol	Meaning
$\bar{U}$	Average tangential force of downstroke
$U^* = C_u/\lambda^2$	Relative tangential force
H	Vertical, upward-directed force component

### Forces During Stroke Cycle

If we assume that flight, analyzed on the basis of the principles presented by Oehme and Kitzler (1974), is determined by average values of the kinematic parameters of the wing strokes, and if it is also assumed that the aerodynamic forces generated during this flight are the same in each stroke cycle, the equilibrium condition can be formulated as follows: over a complete stroke cycle, the sum of the accelerations due to all vertical and horizontal forces is equal to zero. If we can exclude all forces from our power calculation except the vertical forces lift and weight, the thrust-drag problem can then be ignored. It will now be demonstrated how the "motor power" of the bird can eventually be derived from the vertical forces lift and weight.

Lift, which compensates for weight, is not constant over a stroke cycle, and instead there is periodic upward and downward acceleration. Nevertheless, the trajectory of the center of gravity of the body of the bird deviates so little from a straight line that the aerodynamic forces generated by the vertical translations can be neglected, and these minor motions treated as vertical lifting and free fall.

Suppose we are given lift during downstroke and upstroke as a function of time  $[H(t)]$ . Then (Fig. 1): /429

$$\int_{t=0}^{t_{ab}} H(t) dt + \int_{t=t_{ab}}^{t_{gr}} H(t) dt + G t_{gr} = 0$$



Lift has a positive sign, and weight a negative sign. The variable  $H$  is replaced by a constant average downstroke lift  $\bar{H}_{ab}$  and a constant average upstroke lift  $\bar{H}_{auf}$ :

$$\bar{H}_{ab} = (1/t_{ab}) \int_{t=0}^{t_{ab}} H(t) dt; \quad \bar{H}_{auf} = [1/(t_{ges} - t_{ab})] \int_{t=t_{ab}}^{t_{ges}} H(t) dt.$$

Consequently  $\bar{H}_{ab} t_{ab} + \bar{H}_{auf} (t_{ges} - t_{ab}) = G t_{ges}$

and  $\bar{H}_{ab} = [G t_{ges} - \bar{H}_{auf} (t_{ges} - t_{ab})] / t_{ab}$ .

Using the relative downstroke time  $t_{ab}/t_{ges} = y$  and the ratio  $\bar{H}_{auf}/\bar{H}_{ab} = x$  commonly obtained for the average downstroke lift  $\bar{H}_{ab} = |G|/(x + y - xy)$ . The value of  $x$  is between zero and one, and the following three possibilities will be used:

$$\begin{array}{ll} \bar{H}_{auf} = 0 & \bar{H}_{ab} = |G|/(t_{ab}/t_{ges}) \\ \bar{H}_{auf} = 0.5 \bar{H}_{ab} & \bar{H}_{ab} = 2 |G|/(1 + t_{ab}/t_{ges}) \\ \bar{H}_{auf} = \bar{H}_{ab} & \bar{H}_{ab} = |G|. \end{array}$$

We wish to obtain the power of the descending wing from the average downstroke lift. For this purpose, the processes in the wing itself must be examined more closely.

#### Steady-state Rotating Propeller as Model for Downstroke

Since the extended wing sweeps out a circular sector during the downstroke, a logical approach is to utilize the force and power calculation for an air screw. There are, /430 however, differences between a propeller and a pair of flapping wings, and the effects of these differences must be kept in mind

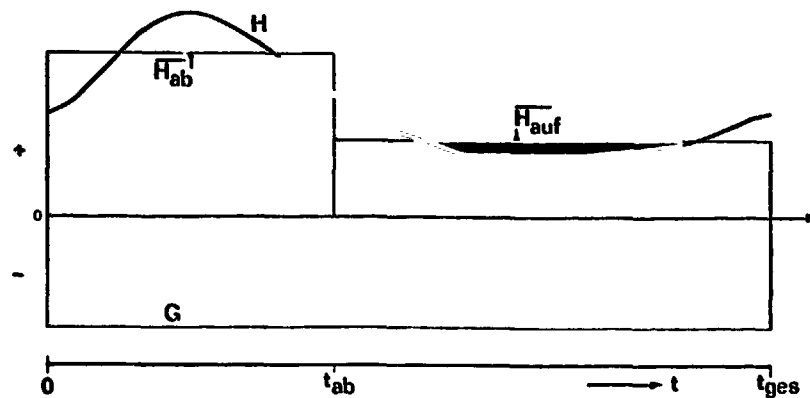


Fig. 1. Schematic of vertical forces during stroke cycle as a function of time:  $t_{ab}$  = duration of downstroke,  $t_{ges}$  = duration of total wing stroke (see text).

when the procedure is applied to the avian wing. Two assumptions for the air screw calculation deserve particular attention: the envisaged procedure describes a propeller moving with constant rate of revolution and constant flight speed. The blades of the propeller rotate in the same direction and maintain the same positions relative to one another.

The downstroke motion starts and ends in each stroke cycle. Moreover, the wing does not rotate with constant angular velocity during the entire downstroke (Oehme and Kitzler 1974). In our thought experiment, we will neglect the acceleration phase of the downstroke motion and assume a constant angular velocity for the entire downstroke. If the tangential velocity  $\omega R$  is large in comparison with the flight velocity  $v$ , as in the case of the airplane propeller, this means large sudden changes in relative air speed for the wing, and enduring effects on flow. All findings to date on horizontal flight, however, indicate

that the velocity ratio  $\lambda = v/(\omega R)$  is no less than one, and larger in most cases. For  $\lambda = 1$ , the effective relative air speed at the wing tip would be about  $1.4v$ , and would otherwise differ even less from the flight velocity.

In the last part of the upstroke, the wing is folded into the air stream (see Oehme 1969b), so that before rotary motion commences, the air approaches the wing with a local velocity equal to the flight speed, which is assumed to be constant, and results in normal circulation around the wing. The rotary motion of the downstroke commences with an acceleration phase. Because of the slight increase in relative air speed, which is not abrupt as opposed to the above assumption, we can suppose that the aerodynamic forces generated on an arbitrary wing section are determined at any time during the downstroke by the parameters valid for the steady-state case (angle of attack, profile polar curve, effective relative air speed). At the transition to the upstroke, circulation does not cease suddenly, but is instead modified by changes in pinion position followed by lifting and, to some extent, folding of the inner wing. Circulation reversals, as observed for hummingbirds or insects hovering with large wing torsion, do not occur. The reduced frequencies (Oehme and Kitzler 1975) calculated for various species likewise lead to the same result: under the conditions of normal, unaccelerated horizontal flight, unsteady effects can be ignored in the treatment of wing circulation.

#### Glauert's (1935) Principle of Airscrew Calculation and its Modification

With velocity  $w$ , air approaches an arbitrary blade element (= wing element) of the propeller at the angle of advance  $\phi$  (Fig. 2).  $\phi$  and  $w$  are determined by the two velocities  $v$  and

$w$ , allowing for the induced velocities in the axial (a) and tangential (b) directions. A normal force, or (following the technical convention) lift  $A$  is produced at right angles to  $w$ , and a drag  $W$  is produced parallel to  $w$ . The resultant aerodynamic forces are decomposed into a component in the flight direction (thrust  $S$ ) and a component at right angles to it (tangential force  $U$ ). The coefficients  $c_s$  (for thrust)<sup>1</sup> and  $c_u$  (for tangential force) are obtained from  $\phi$  and the profile polar curves (coefficients  $c_a$  and  $c_{wp}$ ):

/431

$$\begin{aligned}
 c_s &= c_a \cos \phi - c_{wp} \sin \phi = c_a (\cos \phi - \epsilon_p \sin \phi), \\
 c_u &= c_a \sin \phi + c_{wp} \cos \phi = c_a (\sin \phi + \epsilon_p \cos \phi).
 \end{aligned}$$

The "fullness" of the blade element is  $\sigma = m l / (2\pi r)$ . For  $m = 2$ , we obtain  $\sigma = (l/R) / [(r/R)\pi]$  by introducing the dimensionless quantities  $l/R$  and  $r/R$ . The coefficients for the additional velocities are found from

$$\begin{aligned}
 b/(1-b) &= \sigma c_u F / (4 \sin \phi \cos \phi), \\
 a/(1+a) &= \sigma c_s F / (4 \sin^2 \phi)
 \end{aligned}$$

with  $F = (2/\pi) \arccos e^{-f}$  and  $f = [m(1 - r/R)] / [2(r/R) \sin \phi]$ .  $F$  makes approximate allowance for the number of airscrew blades. The degree of advance is

$$\lambda = (r/R) \tan \phi (1 - b) / (1 + a).$$

The thrust and torque components are

---

<sup>1</sup>The thrust coefficient should not be confused with the thrust loading coefficient, likewise indicated by  $c_s$ , common in German-language literature.

$$\begin{aligned}
R(dC_a/dr) &= \sigma(r/R)^2 (1-b)^2 c_a (1/\cos^2 \Phi) \\
&= \sigma(r/R)^2 (1+a)^2 \lambda^2 c_a (1/\sin^2 \Phi) \\
R(dC_m/dr) &= \sigma(r/R)^4 (1-b)^2 c_a (1/\cos^2 \Phi) \\
&= \sigma(r/R)^4 (1+a)^2 \lambda^2 c_a (1/\sin^2 \Phi).
\end{aligned}$$

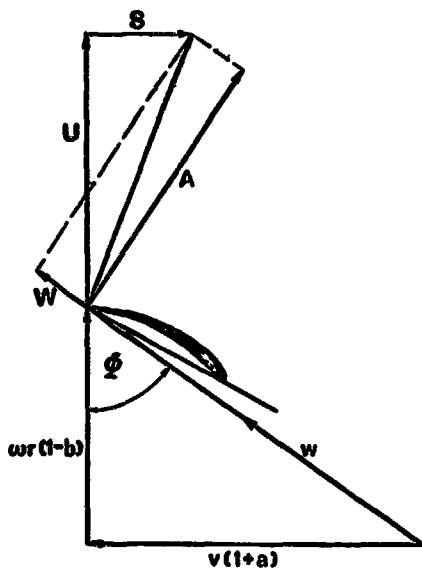


Fig. 2. Components of velocity and force for wing element ( explanation in text).

Given the geometry of the airscrew (chord depth distribution, pitch, profile), we can calculate the thrust and torque elements for various angles  $\Phi$  and for selected blade elements.  $\Phi$  and the pitch of the blade element determine the angle of attack and thus the coefficients  $c_a$  and  $c_{wp}$  fixed in the profile polar curves. With  $c_s$  and  $c_u$  we can obtain  $a$  and  $b$  and then the velocity ratio  $\lambda$  associated with  $\Phi$ . For each of these blade elements, the components of thrust and torque are plotted against  $\lambda$  and determined for particular values of  $\lambda$ . These yield the distributions of thrust and torque components vs.  $r/R$  for a given velocity ratio.

Integrating these curves yields the thrust coefficient  $C_s$  and the torque coefficient  $C_m$  of the propeller for these velocity ratios. (For the quantities customary in German-language literature, we have the relationships  $C_s = 0.5 k_s$ ,  $C_m = 0.5 k_d$ .  $k_s$  is called the thrust parameter, and  $k_d$  the torque or power parameter.) The thrust and torque of the propeller are  $S = C_s \pi \rho \omega^2 R^4$ , and  $M = c_m \pi \rho \omega^2 R^5$ ; the power

is  $P = M\omega = C_m \pi \rho \omega^3 R^5$ . Also,  $c_a$  and  $c_p$  can be given for the individual radial coordinates, assuming that the propeller blade /432 has the corresponding geometric properties. By analogy with the thrust coefficient, we can introduce the tangential force coefficient  $C_u$ . The tangential force element is then  $R(dC_u/dr) = \sigma(r/R)^3(1-b)^2 c_u(1/\cos^2 \phi) = \sigma(r/R)(1+a)^2 \lambda^2 c_u(1/\sin^2 \phi)$ . Power is obtained from torque and angular velocity. Torque can also be formulated with the aid of tangential force and its point of application on the airscrew radius (= wing length)  $R$ , the so-called effective radius. If the effective radius is  $r_z$ , its radial coordinate is  $z = r_z/R$ . The power for one of the two propeller blades is  $0.5 P = 0.5 U R z \omega$ , and thus  $P = U R z \omega$  for the airscrew. Since  $U = C_u \pi \rho \omega^2 R^4$  and  $P = C_m \pi \rho \omega^3 R^5$ , we have  $z = C_m/C_u$ .

This procedure does the job for typical airplane propellers. For the latter, the velocity ratio is small, while the chord depth (and thus the proportion of the circumference covered by the wing elements) is small (cf. Fig. 3). The situation is different for avian wings: large velocity ratios must be allowed for, and chord depth becomes very large near the body. It is evident that the larger the desired velocity ratio, the further out the wing will be the point at which the velocity ratio which can be achieved with the two parameters  $a$  and  $b$  no longer reaches the necessary size. For  $\phi = 90^\circ$ , however, the expression for  $\lambda$  becomes meaningless. This "angle of advance" must, however, be assumed for the critical case: from this wing element inward, the air will approach the wing effectively only from the front. Conditions will then be approximately the same as for the airfoil. The additional /433 tangential velocity acting in the plane of rotation would now have to be replaced by the induced velocity of the airfoil. The system of equations for the propeller, however, cannot represent it. Instead of thrust, there will now be drag in

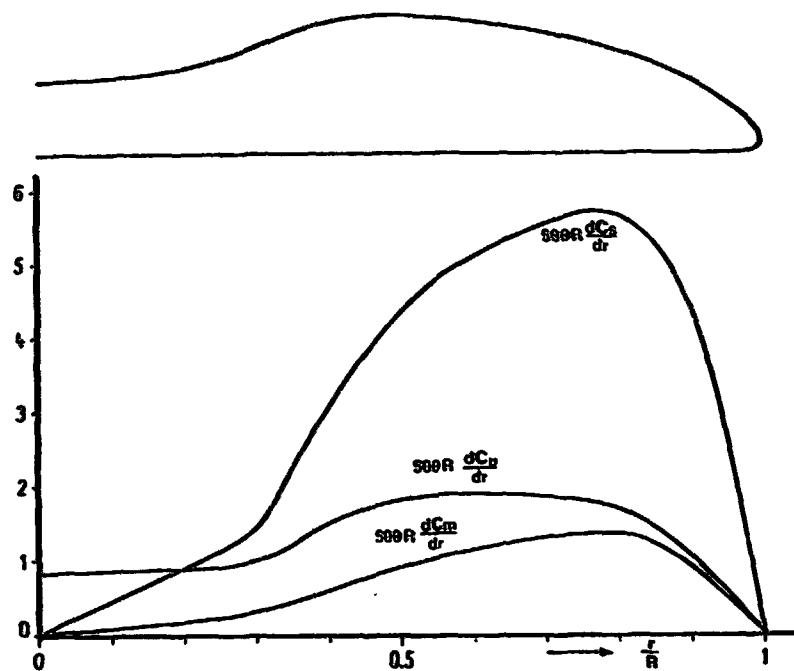


Fig. 3. Wing outline and distribution of elements of tangential force, torque, and thrust for a two-bladed airscrew with velocity ratio  $\lambda = 0.175$ . Modified from Glauert (1935).

the opposite direction. While the angle  $\phi$  corresponding to the desired velocity ratio can be determined for wing elements lying further out, and the components of thrust, tangential force, and torque can be determined from it, they must be considered given data from the critical wing element on, using  $\phi = 90^\circ$ . In that case,  $c_s = -c_{wp}$ ,  $c_u = c_a$ , and

$$\begin{aligned} a/(1+a) &= -\sigma c_{wp} F/4, \\ R(dC_t/dr) &= -\sigma(r/R)(1+a)^2 \lambda^2 c_{wp}, \\ R(dC_u/dr) &= \sigma(r/R)(1+a)^2 \lambda^2 c_a, \\ R(dC_m/dr) &= \sigma(r/R)^2 (1+a)^2 \lambda^2 c_a. \end{aligned}$$

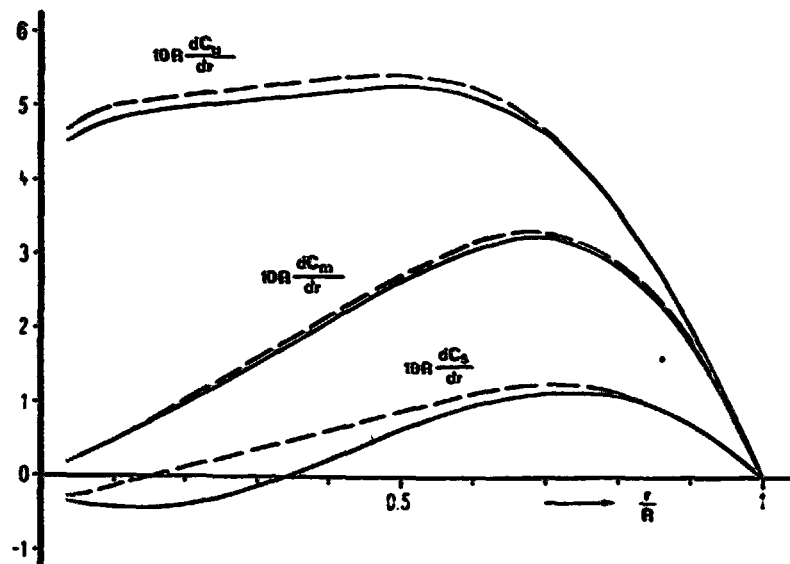
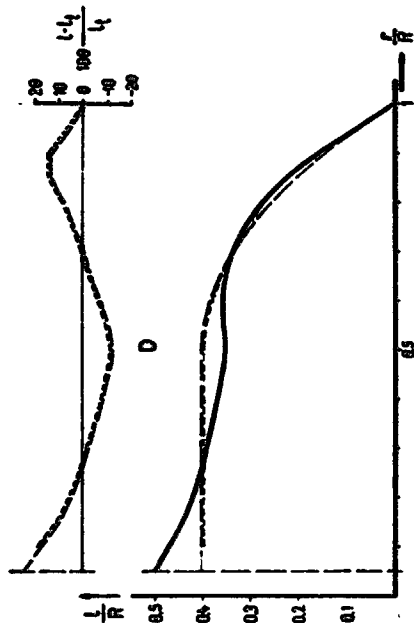
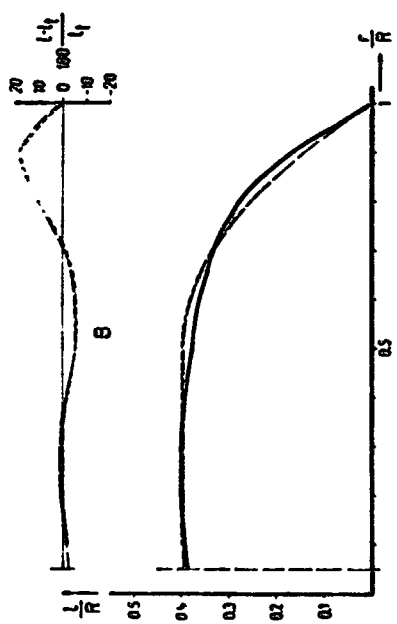
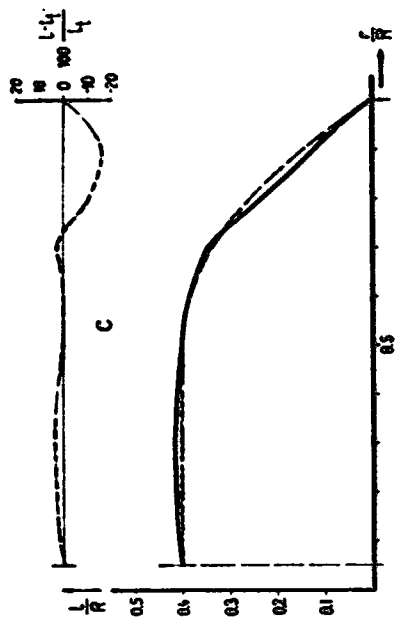


Fig. 4. Distribution of elements of tangential force, torque, and thrust for a two-bladed airscrew with velocity ratio  $\lambda = 1.5$ . Chord depth distribution:  $1/R = 0.4$  for  $0.05 \leq r/R \leq 0.5$ ;  $1/R = 1.6 - (r/R)(1 - r/R)$  for  $0.5 \leq r/R \leq 1$ . Coefficients:  $c_a = 1.0$ ,  $c_{wp} = 0.08$  for  $0.05 \leq r/R \leq 1$ . Solid curves: calculation with supplemental axial and tangential velocities, broken curves; calculation without additional tangential velocity ( $b = 0$ ).

With these approximations, the characteristics of "avian wing propellers" can be ascertained even at large velocity ratios (see Fig. 4). A simplification was sought, in order to avoid having to check along the wing for the critical wing element. It was important that it was not necessary to determine the thrust. Through some comparison calculation, it was established that  $C_m/C_u = z$  remains true, just as in the case of the propeller, if the tangential factor  $b$  is neglected. It is true that  $C_m$  and  $C_u$  now have larger absolute values, but this simpler way is just as good as long as the thrust coefficient is not required (cf. Fig. 4). Determining the effective radius is just





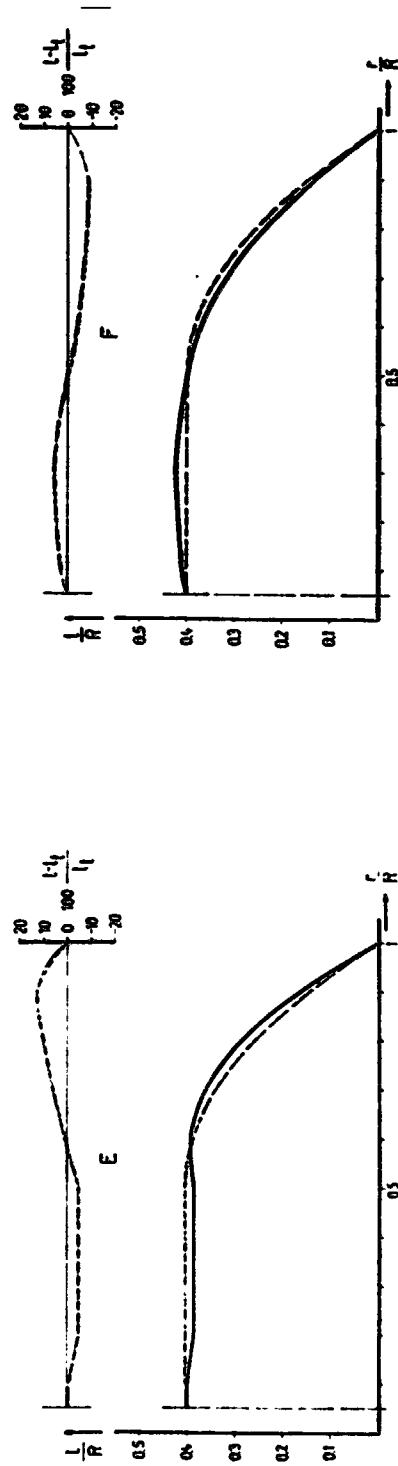


Fig. 5. Chord depth distribution of five wing forms B-F for the variant b. Bottom: chord depth distribution (solid curve) and theoretical chord distribution of a wing of equal area for the case  $\alpha$  (long dashes) and for the case  $\beta$  (short dashes). Top: deviation of chord depth distribution from theoretical chord depth distribution for the cases  $\alpha$  and  $\beta$ . Also see the text.

one problem, however. The second problem is to derive the relationship between downstroke lift and tangential force. As will be shown, the crucial factor is not the absolute magnitude of tangential force, but instead the ratio of the tangential forces for various velocity ratios. This tangential force ratio also proved to be virtually identical in both methods, so that the tangential forces obtained by the simplified calculation could be used in handling this question. /436

#### Location of Effective Radius

The problem is to determine  $z$  as properties of the wing and the velocity ratio are varied, for a two-bladed propeller with chord depth distributions found for avian wings. The various wings will be labelled by a four-part symbol on the following pattern  $Aa \propto 1$  (see Table 1 and Fig. 5).  $R(dC_u/dr)$  and  $R(dC_m/dr)$  were calculated for all integer and half-integer  $r/R$  between  $r_K/R$  and 0.95, with  $\tan \phi = x/(r/R)$ ,  $x \in \{1, 1.5, 2, 3, 5, 7\}$ . From the resulting six pairs of values for velocity ratio and tangential force element or torque element,  $R(dC_u/dr)$  and  $R(dC_m/dr)$  of the wing element were calculated with the aid of a quadratic approximation function for all integer and half-integer  $\lambda$  from one through seven. Then the propeller coefficients  $C_u$  and  $C_m$  were calculated for each of the  $\lambda$  values listed. /437

TABLE I. DESIGNATION OF WING PROPERTIES OF TWO-BLADED AIRSCREW

	Symbol	Meaning
Chord depth distribution	A	Theoretical distribution
	B	Streptopelia decaocto see Fig. 3
	C	Pica pica and
	D	Anas platyrhynchos Oehme and
	E	Larus ridibundus Kitzler
	F	Sturnus vulgaris (1975)

	Symbol	Meaning	
Maximum relative chord	a	$l_{\max}/R = 0.25$	For B-F, this holds
depth, slenderness	b	$l_{\max}/R = 0.40$	for the theoretical
	c	$l_{\max}/R = 0.55$	wings of equal area ( $\alpha$ )
Body contour	$\alpha$	$r_K/R = 0.05$	
	$\beta$	$r_K/R = 0.10$	
Aerodynamic force	$c_a = 0.5, c_{wp} = 0.03$	for $(r_K/R) \leq (r/R) < 1$	
coefficients on wing	$c_a = 1.0, c_{wp} = 0.08$	for $(r_K/R) \leq (r/R) < 1$	
elements	$c_a = 0.65$	for $(r_K/R) \leq (r/R) \leq 0.4$	
	$c_a = 0.65 - 0.5[(r/R) - 0.4]$	for $0.4 \leq (r/R) < 1$	
	$c_{wp} = 0.04$	for $(r_K/R) \leq (r/R) < 1$	

The result can be summarized as follows (see Figs. 6 and 7).

The curves  $z(\lambda)$  of all wings, except for  $[D(\ )\beta(\ )]$ , can be made to coincide with the Abal curve by vertical translation, as long as deviations of up to 0.5% from the values on this reference curve are permitted. The location of the effective radius almost always exhibits the same functional relationship to the velocity ratio, except for one additive parameter.

The influence of aspect ratio can be neglected. In all cases, the difference of  $c$  and  $a$  from  $b$  is at most  $\pm 0.15\%$ .

The variation in  $z$  with increasing  $r_K/R$  can be satisfactorily approximated by a simple relation. For  $r_K/R > 0.05$ , we take  $z = z_a + 0.5r_K/R - 0.025$ . In case  $\beta$ , the resulting value of  $z$  is 0.2%-0.4% too large at  $\lambda = 1$ , and 0.1%-0.2% too large at  $\lambda = 3$ . For wing E, the discrepancy at  $\lambda = 3$  is at most /438 -0.1%. Only for wing D does the discrepancy reach the 1%-limit at  $\lambda = 1$ , due to the abrupt change in chord depth between  $r/R = 0.1$  and  $r/R = 0.05$ ; the approximate values are too small.

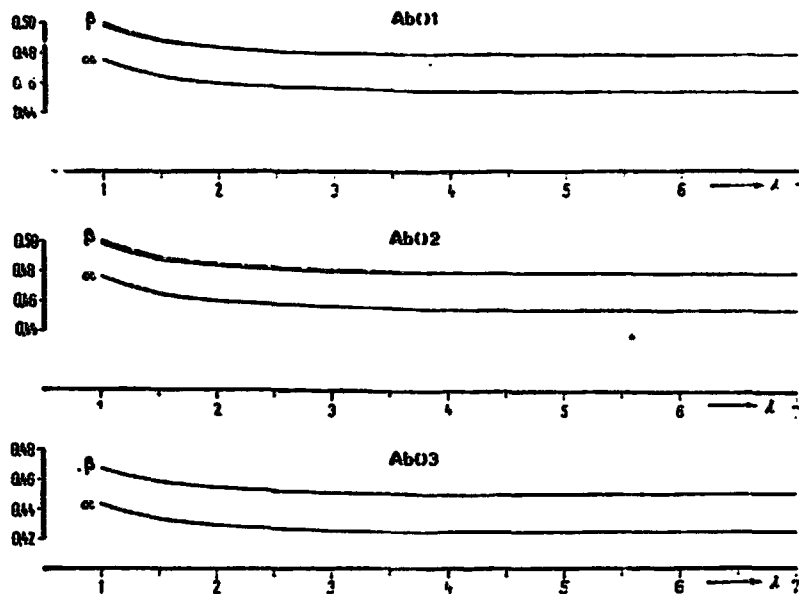


Fig. 6.  $z(\lambda)$  for the wing Ab for different body contours ( $\alpha$ ,  $\beta$ ) and various coefficient distributions (1, 2, 3). Broken parts of curve:  $z$  calculated for  $\beta$  with approximate formula (see also text).

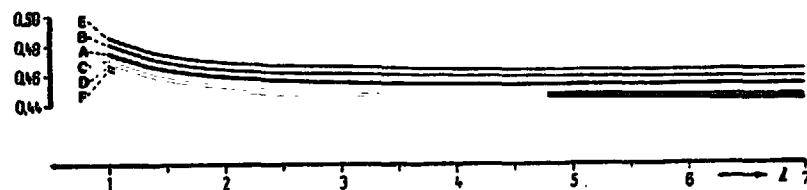


Fig. 7.  $z(\lambda)$  for wing of type ( ) bal for chord depth distributions A-F.

If, when the coefficients are selected for the wing elements, the profile drag-lift ratios  $\epsilon_p = c_{wp}/c_a$  are close enough, the discrepancies in  $z(\lambda)$  will be slight. Thus, the  $z$ -curve in 1 coincides sufficiently with that of 2. And the same result

is obtained as in 3, when the calculations were performed with constant  $c_{wp} = 0.05$  and  $c_a = 0.8$  in place of  $c_a = 0.65$  for the inner wing element. The coefficient distribution of 1 and 2 as compared with 3 causes an increase in  $z$ . In 3, the  $z$ -values are about 93.4% of the values in 1. The coefficients for a flapping wing are not known. For steady gliding flight, an elliptical lift distribution is not unlikely (Oehme 1971). While the chord depth distribution is not elliptical, it does not differ fundamentally from such a distribution, so that there is something to be said for the assumption of constant  $c_a$  over the length of the wing. Whether this holds for flapping flight as well is an open question. The case described here, with  $c_a$  decreasing toward the wing tip, is even more hypothetical. It was introduced merely as a conceivable alternative to constant  $c_a$ , although it is difficult to imagine how such a wing could generate the necessary thrust at high velocity ratios.

The effect of a chord depth distribution (B-F) differing from that of the theoretical wing (A) is not the same in all cases, but on the whole relatively slight for differences of the magnitude considered here (Fig. 5). The largest differences as compared with A are exhibited by E ( $\approx +3\%$ ) and F ( $\approx -3\%$ ). For certain chord depth distribution types, the values of  $z$  can be adequately corrected by using the curves in Fig. 7.

Hence, in calculating the effective radius valid for a particular velocity ratio, one can start from the values for wing Abal as a standard, and correct these values in accordance with the relevant differences (chord depth distribution, body contour, other coefficients)<sup>2</sup>.

---

<sup>2</sup>The standard values  $z(\lambda)$  will be supplied by the authors on request.

### Converting Average Downstroke Lift to Tangential Force

In a previous discussion, only the pitch of the screw jet was neglected in calculating the effective radius. Otherwise, the calculations were made as for a propeller. For the latter, which is there just to generate forward thrust, the tangential force is a necessary evil, and the smaller the tangential force in comparison with the thrust generated, the more economically the propeller operates. The tangential forces produced on the blades of an airscrew cancel out, so that they do not have any effect on the aircraft.

On the other hand, in the case of beating wings "rotating" in opposite directions, the tangential forces produced upon them will have a vertical force component, lift, which will depend on wing position. If the tangential forces on each of the two wings are the same as on the two propeller blades (given the same wing geometry and identical kinematic conditions), /439 the lift generated during the downstroke can be obtained from the tangential force in the propeller model. This presumes that the constantly changing relative position of the wings does not cause any interference. If the beating angles are not too large, this hypothesis will be valid. However, if the wings come close to one another at the beginning and at the end of the downstroke, circulation around the wing will be modified at those points. Hence, the tangential forces, and thus the lift, derive from the propeller model will no longer apply exactly. Consequently, in the sequel, such results will have only limited validity and are utilized primarily for comparison, when the extreme wing angles  $\phi_0$  or  $\phi_u$  exceed  $+65^\circ$  or  $-65^\circ$  respectively. This restriction does not play any role in real cases as will be seen later.

First let us consider the lift yield for the unaccelerated rotary motion of the wing assumed so far. Between times  $t_1 = 0$

and  $t_2$  the wing will traverse the angle  $\phi_1 - \phi_2$  with angular velocity  $\omega$ . Suppose also that tangential force does not change during this time (Fig. 8). In that case, the lift at any time is  $H = U \cos \phi$ , where  $\phi$  is the wing angle at time  $t$  ( $t_1 = 0 < t < t_2$ ). Also,  $\phi = \phi_1 - \omega t$ , and consequently  $\omega t_2 = \phi_1 - \phi_2$  (angle in radians). The change in momentum generated by the variable lift is

$$\begin{aligned} \Delta p &= \int_{t=t_1=0}^{t_2} U \cos(\phi_1 - \omega t) dt = U(\sin \phi_1 - \sin \phi_2)/\omega \\ &= U t_2 (\sin \phi_1 - \sin \phi_2)/(\phi_1 - \phi_2) \end{aligned}$$

since  $\omega = (\phi_1 - \phi_2)/t_2$ . The average lift  $\bar{H} = U (\sin \phi_1 - \sin \phi_2)/(\phi_1 - \phi_2)$ .

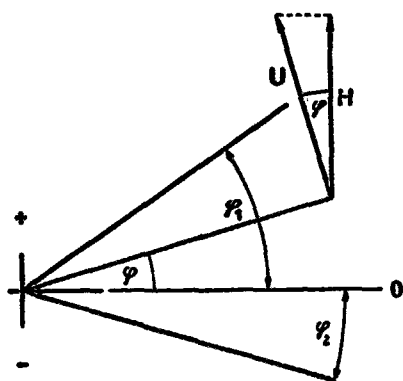


Fig. 8. Principle for calculating lift from tangential force (see text).

Ordinarily, at the beginning of the downstroke, the wing will be accelerated uniformly from  $\omega = 0$  to  $\omega = \omega_{\max}$  during the time  $t = 0$  to  $t = t_b$ , while the wing traverses the angle  $\phi_0 - \phi_b$ . Thereupon it covers the angle  $\phi_b - \phi_u$  with constant angular velocity  $\omega_{\max}$  up to the time  $t_{ab}$ . The ratio of average tangential force to average lift is then

/440

$$\bar{U}/\bar{H}_{ab} = \int_{t=0}^{t_{ab}} U(t) dt / \int_{t=0}^{t_{ab}} H(t) dt.$$

The integral is evaluated as above for the time interval  $t_{ab} - t_b$  and by approximation for the interval between  $t = 0$  and  $t = t_b$ .



Because of the relation  $t_{ab} = t_b (n + 1)$ ,  $\omega_{\max} = (\phi_b - \phi_u)/(t_{ab} - t_b)$  and  $\phi_b = \phi_0 - 0.5 \phi_{\max} t_b$ , we obtain  $t_b = (\phi_0 - \phi_u)/[\omega_{\max} (n + 0.5)]$ . Also, the constant angular acceleration is  $\alpha = \omega_{\max}/t_b$ . At time  $t_1$  ( $0 < t_1 \leq t_b$ ), the angular velocity is  $\omega_1$ . Therefore,  $t_1 = \omega_1/\alpha = \omega_1 t_b/\omega_{\max}$ . At an angular velocity of  $\omega_1$ , the velocity ratio is  $\lambda_1 = v/(\omega_1 R)$ . Therefore,  $\omega_1 = v/(\lambda_1 R)$ . Since  $\omega_{\max} = v/(\lambda_{\min} R)$ , we have  $t_1 = \lambda_{\min} t_b/\lambda_1$ . Dividing by  $t_{ab} = t_b (n + 1)$  yields the relative times  $\tau_1 = t_1/t_{ab} = \lambda_{\min}/[\lambda_1 (n + 1)]$ . At time  $t_1$ , the wing angle is  $\phi_1 = (\phi_0 - \phi_u - \omega_1 t_1)/2 + \delta$ . At  $t_1 = \lambda_{\min} t_b/\lambda_1$ , we find  $\phi_1 = 0.5 (\phi_0 - \phi_u) \{1 - \lambda_{\min}^2/[\lambda_1^2 (n + 0.5)]\} + \delta$ . Thus,  $\tau_1$  and  $\phi_1$  can be calculated during acceleration for given  $\lambda_{\min}$  and  $n$ , for arbitrarily many velocity ratios  $\lambda_1$ .

The average tangential force ( $\bar{U}$ ) and the average downstroke lift ( $\bar{H}_{ab}$ ) are obtained as follows.

$$\bar{U} = \int_{\tau=0}^1 U(\tau) d\tau \quad \begin{array}{l} \text{numerically for } 0 \leq \tau \leq \tau_b, \\ \text{in closed form for } \tau_b \leq \tau \leq 1 \end{array}$$

$$\int_{\tau=\tau_b}^1 U(\tau) d\tau = U_{\max} (1 - \tau_b) = U_{\max} \cdot n/(n + 1);$$

$$\bar{H}_{ab} = \int_{\tau=0}^1 H(\tau) d\tau \quad \begin{array}{l} \text{numerically for } 0 \leq \tau \leq \tau_b \\ \text{with } H_1 = U_1 \cos \phi_1, \\ \text{in closed form for } \tau_b \leq \tau \leq 1 \end{array}$$

$$\int_{\tau=\tau_b}^1 H(\tau) d\tau = [U_{\max} (\sin \varphi_b - \sin \varphi_u)/(\varphi_b - \varphi_u)] \cdot n/(n + 1)$$

The conversion factor for lift into tangential force is  $k(\phi_0 - \phi_u; \delta; n; \lambda_{\min}) = \bar{U}/\bar{H}_{ab}$ .

Instead of calculating with the tangential forces of specific wings at specific angular velocities, one can use the tangential force coefficient  $C_u$ .  $U = C_u \pi \rho \omega^2 R^4$ . With  $\omega = v/\lambda R$ , we obtain  $U = C_u \pi \rho v^2 R^2 / \lambda^2$ . Since  $v$  is being assumed constant,  $\lambda$  varies only when  $\omega$  does. Hence,  $U = (C_u \cdot \text{const}) / \lambda^2$ . The relative tangential force  $U^*$  is substituted for  $U/\text{const}$ . For arbitrary  $\lambda_1$ , we have  $U_1^* = C_{u1} / \lambda_1^2$ , and  $H_1^* = U_1^* \cos \phi_1$ .

The "tangential force" for  $\tau = O(U_0)$ , i.e.  $\phi_0$ , can be obtained with sufficient accuracy from graphs of the function  $U^*(\lambda)$  by extrapolation to large values of  $\lambda$ .

$U^*$  was determined for all integer and half-integer values of  $\lambda$  from one to seven for the same wings as in the  $z$ -calculation. The value of  $U^*$  at  $\lambda = 2$  was taken to be unity and all other  $U^*$  values expressed in this unit (Fig. 9).

/441

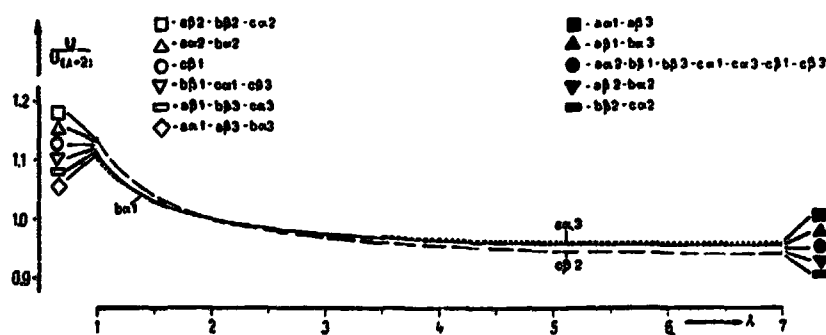


Fig. 9. Tangential force as a function of  $\lambda$  for the wing A (see text).

The deviations from wing Ab01 are small throughout. Changes in chord depth distribution on the scale utilized here (B-F) have virtually no effect, while changes in the aerodynamic coefficients and in the aspect ratio have detectable effects, as do, on a smaller scale, changes in the position of the body

contour. The values of  $k$  were calculated for the wing Aba1 at  $\lambda_{\min} = 2$ , and for the flapping angles  $(\phi_0 - \phi_u)$   $60^\circ, 70^\circ, 80^\circ, \dots, 140^\circ$  with angles of asymmetry  $(\delta)$   $-10^\circ, -5^\circ, 0^\circ, 5^\circ, 10^\circ$  and with the time factors  $(n)$  2, 3, 4, 5, 10,  $\infty^3$ .

For the same wing, and for the wings Ac $\beta$ 2 and Aa $\alpha$ 3, whose U-curves deviated most from that of Aba1 (Fig. 9), these  $k$ -values were also determined for  $\lambda_{\min} = 1$  and  $\lambda_{\min} = 3$  for extreme conditions (maximum flapping amplitude, maximum positive angle of asymmetry, maximum relative acceleration time) (Table 2). The error generated in using the standard values is small, even when the initial kinematic values are unfavorable, and does not exceed the 1%-limit for what experience has shown to be normal values  $(\phi_0 - \phi_u \leq 125^\circ, -5^\circ \leq \delta \leq +5^\circ, \text{ and } n \geq 3)$ .

TABLE II. DIFFERENCE BETWEEN  
k AND STANDARD VALUE (Aba1 for  $\lambda_{\min} = 2$ )  
AT  $\phi_0 - \phi_u = 140^\circ, \delta = +10^\circ, n = 2$ .

wing	$\lambda_{\min}$	error (%)
Aba1	1	-1.27
	2	0
	3	+0.14
Aa $\alpha$ 3	1	-1.12
	2	+0.09
	3	+0.21
Ac $\beta$ 2	1	-1.74
	2	-0.2
	3	-0.01

<sup>3</sup>These tabulated standard values are available from the authors on request.

## Influence of Initial Acceleration in Downstroke on Location of Effective Radius

/442

By analogy with the average tangential force, we can calculate the average power:

$$\bar{P} = \int_{\tau=0}^1 P(\tau) d\tau.$$

Here too a relative power can be introduced.  $P = C_m \pi \rho \omega^3 R^5$  implies  $P_i^* = C_{mi}/\lambda_i^3$ . The average angular velocity of the downstroke  $\bar{\omega} = (\phi_0 - \phi_u)/t_{ab} = \lambda_{\max} (n + 0.5)/(n + 1)$  corresponds the average velocity ratio  $\bar{\lambda} = v/\bar{\omega}R = \lambda_{\min} (n + 1)/(n + 0.5)$ . The effective radius is obtained from the relation presented earlier (see p. 11)  $z = \bar{P}/(\bar{U}\bar{\omega}R)$ , or, using the relative values,  $z = \bar{P}^*\bar{\lambda}/\bar{U}^*$ .

For  $n = 2$ , the difference between the resulting value of  $z$  associated with  $\bar{\lambda}$  and the value calculated at constant angular velocity ( $n \rightarrow \infty$ ) is +2.84% at  $\bar{\lambda} = 1.2$  ( $\lambda_{\min} = 1$ ); +0.94% at  $\bar{\lambda} = 2.4$  ( $\lambda_{\min} = 2$ ) and +0.46% at  $\bar{\lambda} = 3.6$  ( $\lambda_{\min} = 3$ ). The larger  $n$  is, the less significant the difference is, so that for time factors  $n \geq 3$ , even for velocity ratios  $\bar{\lambda} \approx 1$ , the 2%-limit is not exceeded.

## Execution of Power Calculation -- Discussion of Method

The average power of the pair of wings during the downstroke was  $\bar{P}_{ab} = \bar{U} \bar{\omega} R z$  by analogy with the power of the propeller  $P = U \omega R z$ .  $\bar{U}$  is determined by the average downstroke lift  $\bar{H}_{ab}$  and the conversion factor  $k$ :  $\bar{U} = \bar{H}_{ab} k$ . Hence,  $\bar{P}_{ab} = \bar{H}_{ab} \omega R z k$ . With one exception, the factors contained in the equation are quantities not measured directly, but instead derived from measured data (see Fig. 10). All are average

values, so that the effects of their errors on the final result must be taken into account. This is accomplished by means of the modifications presented below.

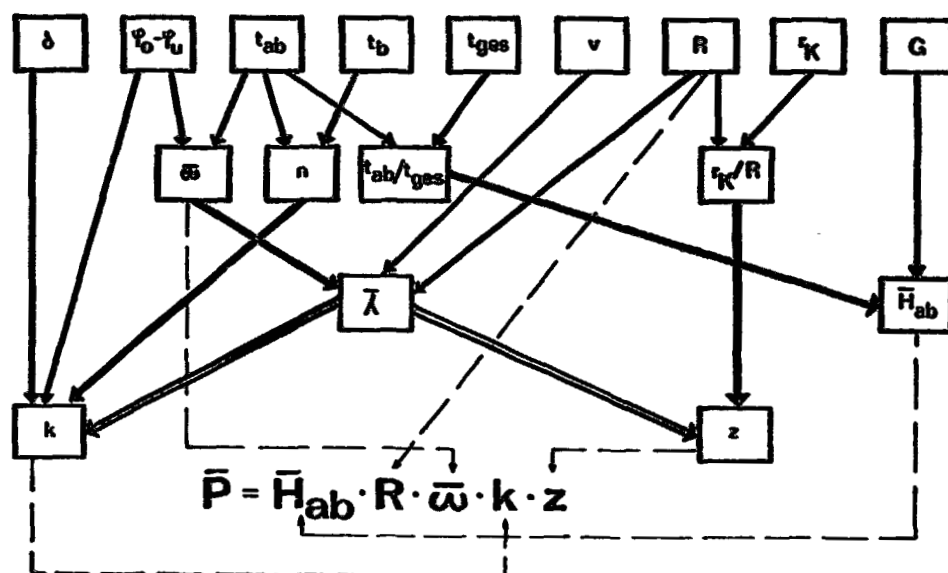


Fig. 10. Connections between measured values and result of power calculation.  
[indices: ad = downstroke; ges = overall]

For each flight analyzed, three calculations were made for /443 a fixed ratio  $\bar{H}_{auf}/\bar{H}_{ab}$ : one for the average value and one for the maximum and minimum possible values. In detail:

Average downstroke lift  $\bar{H}_{ab}$ : obtained from the weight  $G$  and in two cases from the relative downstroke time  $t_{ab}/t_{ges}$ . For  $G$ , it was not the average error, but the largest and smallest values of the series of measurements which was employed. The error interval of the relative downstroke time is obtained from the average errors of  $t_{ab}$  and  $t_{ges}$ .

$$\left[ (G)_{\min}^{\max}, (t_{ab}/t_{gs})_{\min}^{\max} \right] \rightarrow (\bar{H}_{ab})_{\min}^{\max}.$$

Wing length R: if it may be assumed that there is a correlation between G and R for the species involved, which might also be divided by sex<sup>4</sup>, the values of R corresponding to the largest and smallest G on the basis of the correlation were used. When a correlation was unlikely, the average was always employed, i.e. R had no maximum or minimum.

Average angular velocity of downstroke  $\bar{\omega}$ : is derived from the flapping angle  $\phi_0 - \phi_u$  and the downstroke time  $t_{ab}$ :  
 $\bar{\omega} = (\phi_0 - \phi_u) \cdot \pi / (180 \cdot t_{ab})$  with angles in ° and time in seconds. The error interval is obtained from the average errors of the stroke angle and the downstroke time.

$$(G)_{\min}^{\max} \rightarrow \left[ (\phi_0 - \phi_u)_{\min}^{\max}, (t_{ab})_{\min}^{\max} \right] \rightarrow (\bar{\omega})_{\min}^{\max}.$$

Position of effective radius z: determined from standard curve with velocity ratio  $\bar{\lambda}$ , corrected for wing shape, and then converted to final form, using the position of the body contour.

a) Downstroke velocity ratio  $\bar{\lambda} = v/(\omega R)$ :

$$(G)_{\min}^{\max} \rightarrow \left[ (v)_{\min}^{\max}, (\bar{\omega})_{\min}^{\max}, (R)_{\min}^{\max} \right] \rightarrow (\bar{\lambda})_{\min}^{\max} \rightarrow (z_{vorl.})_{\min}^{\max}$$

[vorl. = provisional]

---

<sup>4</sup>This only makes sense when the sexes can be clearly identified, even in flight.

b) Position of body contour  $r_K/R$ : the error interval is obtained from the average errors of  $r_K$  and  $R$ .

$$(G) \begin{matrix} \max \\ \min \end{matrix} \rightarrow \left[ \begin{matrix} \max \\ \min \end{matrix} (z_{\text{vorl.}}), \begin{matrix} \max \\ \min \end{matrix} (r_K/R) \right] \rightarrow \begin{matrix} \max \\ \min \end{matrix} (z)$$

The factor  $k$  for converting average downstroke lift into tangential force: determined with the aid of the time factor  $n$ , the stroke angle  $\phi_0 - \phi_u$ , and the angle  $\delta$  of asymmetry. The values of  $k$  were obtained by linear interpolation in all three tabulated variables.

a) Time factor  $n = (t_{ab}/t_b) - 1$ . The average errors of  $t_{ab}$  and  $t_b$  determine the error interval of  $n$ .

$$(G) \begin{matrix} \max \\ \min \end{matrix} \rightarrow \left[ \begin{matrix} \min \\ \max \end{matrix} (t_{ab}/t_b) \right] \rightarrow \begin{matrix} \min \\ \max \end{matrix} (n) \rightarrow \left[ \begin{matrix} \max \\ \min \end{matrix} (k) \right]$$

b) Stroke angle  $\phi_0 - \phi_u$ .

$$(G) \begin{matrix} \max \\ \min \end{matrix} \rightarrow \left[ \begin{matrix} \max \\ \min \end{matrix} (\phi_0 - \phi_u) \right] \rightarrow \left[ \begin{matrix} \max \\ \min \end{matrix} (k) \right]$$

c) Angle of asymmetry  $\delta$ .

$$(G) \begin{matrix} \max \\ \min \end{matrix} \rightarrow \left[ \begin{matrix} \max \\ \min \end{matrix} (\delta) \right] \rightarrow \left[ \begin{matrix} \max \\ \min \end{matrix} (k) \right]$$

The relationships shown in a) and c) apply for the cases /444  $2 \leq n \leq 5$  and  $-5^\circ \leq \delta \leq +5^\circ$ . For  $\delta < -5^\circ$  and  $n < 5$ , the situation is partially reversed. Nothing can be changed via  $n$ , however, because the smallest  $n$  is associated with the minimum of  $(t_{ab}/t_{\text{ges}})$  and the maximum of  $\bar{\omega}$ . On the other hand,  $\delta$  is arbitrary and the

values can be selected so that they result in the minimum or maximum  $k$ .

As explained,  $z$  and  $k$  deviate from the standard values, depending on  $\lambda$ . While using  $\bar{\lambda}$  always makes  $z$  too small,  $k$  is too large at small values of  $\lambda$ . The errors cancel to some extent. The product  $kz$  is always a bit too small, at worst by about 2%, but usually by less than 1%. At any rate, using the standard values does not result in a power which is too large, so that a correction can be omitted. A sufficiently close approximation for velocity ratios between 1 and 1.5 is raising the power found with the aid of the standard values by 1%.

The sources of the initial data vary. While the kinematic parameters characterize a specific flight of an individual bird, the morphological parameters derived from series measurements are theoretically characteristics of the (abstract) ideal representative of the species or of a population of the species or of a segment of it, but in reality are approximations obtained from random samples. Therefore, it is best to include, for the time being, the entire range of variation of weight and, if appropriate, wing length in the calculation. The true value for the flight model can then be relatively confidently expected to lie in the interval between the maximum and minimum downstroke powers. The procedure does not supply a precise value for a particular individual, but instead a range of values for the species concerned. The width of the interval will be determined by the accuracy of the initial values, and the significance of the results must be discussed from this viewpoint. Depending on the quality of the primary data, one may obtain only an order-of-magnitude estimate of downstroke power or a precise analysis of e.g. the relationship between flight velocity and power or the flight powers of males and females.



This all holds for our time model of the downstroke: it begins with an acceleration phase, and once the maximum angular velocity has been attained, it is maintained until the end of the downstroke. Downstrokes with varying angular velocity and consequently several acceleration phases would have to be treated individually, and the tabulated conversion factors  $k$  would not be applicable. If the  $\phi(t)$  curve of such a downstroke is replaced by a different one in which all the intervals of acceleration are combined into a single initial acceleration, while the stroke angle and the downstroke time remain unchanged, substitute curves  $\phi(t)$  or  $\omega(t)$  are obtained, for which the time factor  $n$  is then given as well (see Oehme and Kitzler 1974). We will use two examples to show how the application of the method of calculation to such simplified kinematic conditions affects the two factors  $z$  and  $k$  (Fig. 11). Case 1: for the substitute curve,  $\phi_0 - \phi_u = 140^\circ$ ,  $\delta = 0$ ,  $n = 2$ ,  $\lambda_{\min} = 1.5$  at  $\omega_{\max} = 20/\text{sec}$ , /445  $\bar{\lambda} = 1.8$ . Two quite different sequences lead to these substitute values. The separate accelerations combined into a single initial acceleration vary in magnitude and sign. Case 2: for the substitute curve,  $\phi_0 - \phi_u = 140^\circ$ ,  $\delta = 0$ ,  $n = 2$ ,  $\lambda_{\min} = 1$  at  $\omega_{\max} = 20/\text{sec}$ ,  $\bar{\lambda} = 1.2$ . The original three accelerations are equal in magnitude and sign, but occur at different times. Moreover, this is an extreme case in which the rotation of the wing stops completely, whereupon the wing is reaccelerated up to its old angular velocity. The original downstroke was /446 calculated in sections, the relative values of tangential force, average downstroke lift, and average downstroke power obtained by summing over the downstroke time, and the factors  $k$  and  $z$  calculated from these figures. Compared to the standard values (relative to  $\bar{\lambda}$ ), the following differences resulted (Table 3). While  $z$  is the same in Case 2 for the original and the substitute curves, the simplification in Case 1 results in a value which is too small. The  $k$ -values of the originals naturally depend on the position of the accelerations within the downstroke. The

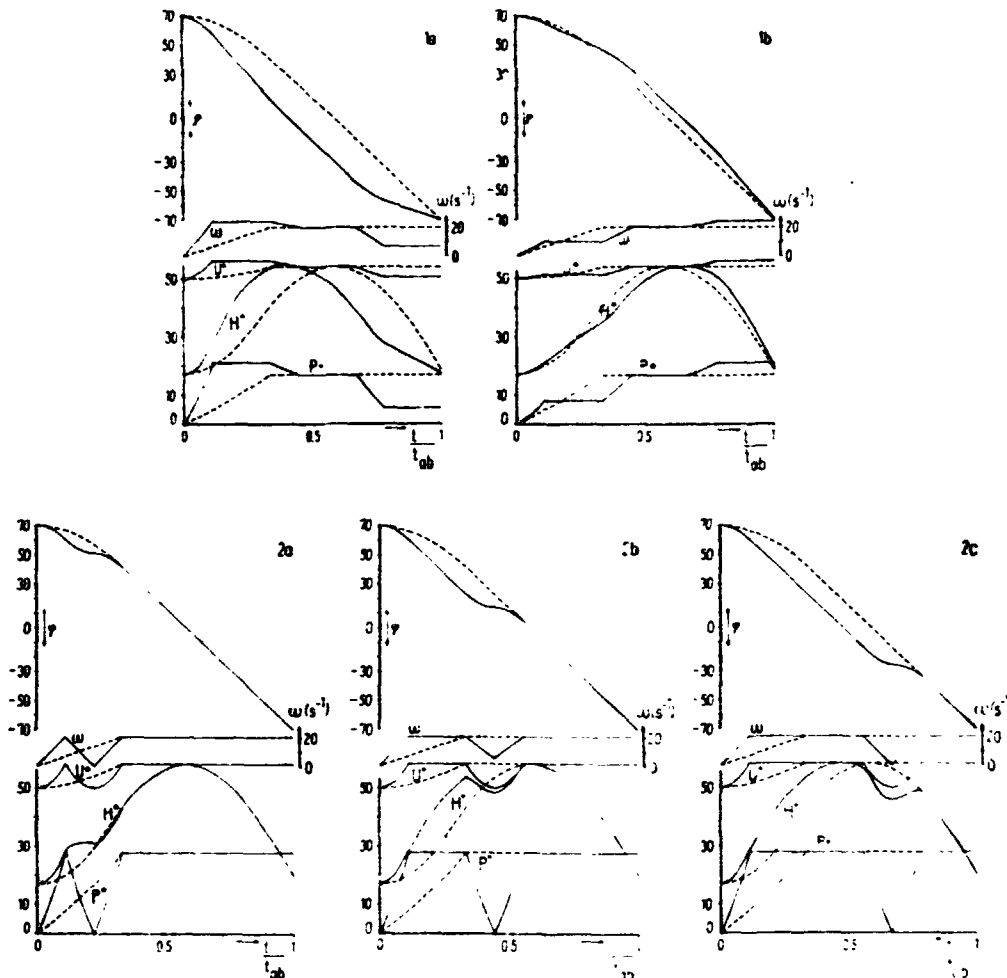


Fig. 11. Tangential force, lift, and power as functions of time for different downstrokes with several periods of acceleration. Solid curves: original downstroke. Broken curves: Substituted downstroke with pure initial acceleration. Wing Abal. (See text for explanation).

complete stoppage of rotation followed by reacceleration (Case 2) has a much greater effect than changes in angular velocity without complete stoppage (Case 1). The calculation with the values of  $k$  and  $z$  corresponding to the substitute curve would yield powers which were too small in Case 1, but too large in Case 2,

TABLE III. DIFFERENCES IN FACTORS  $k$  AND  $z$  FOR THE ORIGINAL AND SUBSTITUTE CURVES  $\phi(t)$  FROM THE STANDARD VALUES (in %)

	Case	1a	1b	2a	2b	2c
$k$	Original	+1.60	-0.61	-2.98	-7.05	-6.47
	Substitute	-0.66		-0.83		
$z$	Original	+2.41	+2.41	+2.84	+2.84	+2.84
	Substitute	+1.26		+2.84		

particularly when the multiple accelerations occur near the angle bisector of the stroke angle. A single irregular wing-stroke, used in obtaining the initial kinematic data via the substitute curve, would hardly falsify the result. However, if "irregular" wing beats are the norm, the calculation will supply only an approximation, and it will have to be estimated whether the result is too large or too small. Nevertheless, the differences will usually be smaller than those in the examples, when the stroke angle is smaller and the time factor larger. If the downstrokes are so irregular that  $n < 2$  for the substitute curve, the calculations will no longer furnish useful results. However, it is quite unlikely that such a case would represent unaccelerated horizontal flight.

Finally, we wish to discuss once more the principles of the procedure. The induced tangential velocity of the propeller was neglected ( $b = 0$ ), since it has practically no effect on the location of the point of application of the total tangential force for the given velocity ratio, and since even the ratio of the tangential forces does not change at different velocity ratios. However, to a specific tangential force must correspond a specific tangential velocity increment or the vertical velocity along the inner parts of the wing corresponding to the downwash. Therefore, if one desires to calculate the tangential force for

a given wing with specified coefficients, assuming this force to be equal to that on the propeller rotating through the entire circular screw surface, the factor  $b$  can be hardly be ignored and an expression for the induced velocity along the inner wing must be introduced (cf. Fig. 3). As the two wings /447 traverse the stroke angle, the additional velocity has a component directed vertically downward and dependent on wing position. This corresponds to the downstroke lift, which varies in the same way, and a mean vertical induced velocity then corresponds to the average downstroke lift. If one wishes to draw inferences about tangential force, and eventually about power, from the momentum of the "flapping wing jet" assigned to this velocity, the stroke-angle-dependent contribution to angular momentum and the time of the downstroke during the stroke must not be ignored. However, any experiment designed in this fashion presumes knowledge of values which are usually not available. The approximation method developed here avoids these difficulties, by permitting the use of any tangential force determined eventually by the weight of the animal, and presuming the existence of the induced velocities corresponding to it, without representing them precisely. Thus, the second force component generated, namely thrust, is not represented. The induced drag on the wing, determined by its aspect ratio, likewise does not appear. Since lower induced drag means greater thrust yield, theory would lead one to anticipate a relationship between calculated powers and flight velocities. When the same power is calculated for two equally heavy birds with equal surface load, the one with the slenderer wing must be faster, assuming that the two birds have the same body drag and the same wing profiles. Pure examples of this case will not occur in practice, without coming up against the unit own force parameters again. However, more extensive comparisons would have to confirm that slow-flying narrow-winged birds have relatively the smallest powers, and fast-flying broad-winged birds the

relatively greatest ones. If this is the way that the effect of any drag reduction due to free primaries (see Oehme and Kitzler 1975) were to be discovered, it would require extremely precise measurements of velocity, because of the smallness of the effect. Consequently, corroboration cannot be expected. For the power calculation itself, the special pinion structure has no influence.

One starting point in the derivation of the effective radius and the conversion factor for lift was the assumption of constant force parameters on the wing elements during the downstroke. A periodic variation in angle of attack, as assumed by von Holst (1943) and von Holst and Kuchemann (1941), would also induce such variations in the force parameters, particularly in  $c_a$ . Tangential force would then depend not only on angular velocity, but also on wing position. This would require further information on the magnitude of the angular changes and thus of the changes in the coefficients, which would again presume precise profile polar curves for the individual wing elements. It is hardly possible to make sufficiently precise measurements of angle on various wing sections when the bird is flying freely. This has been done for a trained bird flying in a wind tunnel (Bilo 1971), but these studies have likewise shown that it is very difficult to monitor a certain period of time over several stroke cycles and to separate wing strokes altered by control movements from "ordinary" ones of powered flight. The theory of von Holst states that the effective angle of attack, increasing from the root to the tip of the wing, reaches its maximum as the wing passes through the horizontal, and has an identical smaller value at the beginning and end of the downstroke at all points on the wing. This means roughly a reversal of the coefficient distribution 3 in the middle of the downstroke. Thus,  $z$  grows from the beginning of the downstroke to the middle of the downstroke, and then decreases again. /448

Converted to a constant average downstroke lift,  $z$  becomes appreciably greater. For the same case,  $k$  becomes somewhat smaller, because the maximum of tangential force coincides with the horizontal wing position ( $\phi = 0$ ,  $\cos \phi = 1$ ). On the whole, the result is a downstroke power greater than in the case of constant coefficients. As far as can be judged by time-lens photographs, the pinion of the wing is pronated during the acceleration phase of the downstroke motion, and then remains in this position during the rest of the downstroke. This would be compatible with the hypothesis of more or less constant coefficients on the wing elements: at the beginning of the downstroke ( $\omega = 0$ ), the entire wing is parallel to the approaching airstream. With increasing angular velocity, the airstream approaches from further and further beneath the wing, and the further the wing section lies from the shoulder joint, the greater the difference between the relative air direction and the longitudinal axis of the bird. Thus, the twisting can preserve the original angle of attack and keep the coefficients, particularly  $c_a$ , roughly constant.

For a typical downstroke (i.e. with purely initial acceleration), all calculations tended to yield powers which were too small. This is in fact an advantage if we are trying to demonstrate just how great the flight power is. The only parameter which is not measured, but instead assigned, is the ratio of upstroke lift to downstroke lift. Any value between the two extremes  $\bar{H}_{auf} = 0$  and  $\bar{H}_{auf} = \bar{H}_{ab}$  is theoretically possible. At this point, we considered only the possibility  $\bar{H}_{auf} = 0.5\bar{H}_{ab}$ . If every concrete case can be classified into one of the two intervals, the upper and lower powers would be obtained. The only difficulty is that forces in this case must be directly estimated from morphological features. However, a rule can be derived from a close examination of the upstroke using kinematographic recording. In many small birds, the wing

is largely folded up during the upstroke. They can readily be assigned to the category  $0 < H_{auf} < 0.5H_{ab}$ . In large birds, the rule is that the pinion is more or less folded and bent toward the inner part of the wing during the upstroke, while the inner half remains unfolded and acts as a lift-generating surface:  $0.5H_{ab} < H_{auf} < H_{ab}$ . The upper limit is probably not reached, because the lift-generating surface is smaller than in the downstroke, and such a large vertical force component could then only be achieved by relatively large angle of attack, producing a great increase in reverse thrust, and eventually the latter could no longer overcome by the thrust generated during the downstroke.

With the present form of the calculating method, the power resulting from the action of the wing on the mass of air which it moves during the downstroke can be obtained. The power /449 required to overcome the inertia of the wing from the beginning of the downstroke is ignored. The calculation also ignores the muscular work performed during the upstroke as well as energy released in other organs. Taking the calculated power simply as flight power, i.e. converting it to the entire stroke cycle has to yield lower values than would a total power determination on metabolic and physiological principles.

## Part II: Specific Power Capacity of Pectoral Muscles of Columbia Livia (pigeon) and Streptopelia Decaocto in Horizontal Flight

### Material

Our method of calculation was applied to two species whose horizontal flight is pure powered flight, and is thus not interrupted by gliding or sailing phases. A population of wild city doves at the edge of the Berlin Zoo and the large population of Turkish doves inhabiting the entire Zoo area provided morphological and kinematic data.

The weight, the weight of the two pectoral muscles, the length of the wing, and the position of the body contour were measured on freshly killed adult animals (see Oehme and Kitzler 1975). In both species, the sexes can generally be distinguished in flight, so that no separate analysis of males and females was carried out. The subjects were 17 pigeons (9 males, 8 females) and 23 Turkish doves (11 males, 12 females). In both species there was a positive correlation between total weight and weight of the pectorals (error probability 5%), while one existed between total weight and wing length only in the Turkish dove. The equations for the regression lines are  $G_{\text{pect}} = 0.0285 + 0.089 G$  and  $R = 0.167 + 0.4 G$  for *Streptopelia* and  $G_{\text{pect}} = 0.021 + 0.1322 G$  for *Columba* ( $G$  and  $G_{\text{pect}}$  in kg,  $R$  in m). In both species, the edge of the body contour is at  $r_K/R = 0.075 \pm 0.001$ . The following values, associated with the smallest, average, and largest  $G$ , were obtained (Table IV). The relative pectoral weight is also listed.

TABLE IV. MORPHOLOGICAL PARAMETERS OF THE TWO SPECIES OF DOVE

	$G$ (kg)	$R$ (m)	$r_K/R$	$G_{\text{pect}}$ (kg)	$G_{\text{pect}}/G$
<i>Columba livia</i>	0.250	0.316	0.074	0.033	0.212
	0.388	0.316	0.075	0.064	0.192
	0.388	0.316	0.076	0.071	0.183
<i>Streptopelia decaocto</i>	0.159	0.231	0.074	0.043	0.270
	0.300	0.247	0.075	0.046	0.230
	0.231	0.259	0.076	0.049	0.212

The film material assembled for both species made it possible to calculate nine pigeon and seven Turkish dove flights. The method by which the kinematic parameters were derived has already been described (Oehme and Kitzler 1974). The downstrokes were all of the ordinary type, with only one



period of angular acceleration. The flight velocity  $v$  could only be determined roughly by measuring the time between known terrain points, allowing for the direction and the strength of the wind. Experiments with models have demonstrated that such a procedure involves an uncertainty of 10% on both sides. This was taken to be the error interval for the velocities of the birds.

## Results and Discussion

/450

The values obtained for power -- specific power of the pectorals and average relative power -- are depicted in Fig. 12. They were calculated for the two extreme cases  $\bar{H}_{auf} = 0.5\bar{H}_{ab}$  and  $\bar{H}_{auf} = \bar{H}_{ab}$ , the upstroke (see Fig. 13) indicating that the first equation is closer to the real situation. During the upstroke, the Turkish dove folds its wings more than does the pigeon. so that for this species, the average upstroke lift is somewhat smaller, which would increase the downstroke. The pigeon was assumed to have the chord depth distribution of the theoretical wing, while the standard values for  $z$  were raised by 1% for the Turkish dove (wing form B)<sup>5</sup>.

We will first discuss relative downstroke power converted to the stroke cycle, because it opens to possibility of a comparison with metabolic-physiological findings. The expression  $(\bar{P}_{ab} \cdot t_{ab}/t_{ges})/G$  would express the average power, relative to body weight, if it were derived only from the pectoral power during the downstroke. Total energy consumption of the bird per time and weight must be higher. Thermal energy per unit of time (kcal/h) is converted to mechanical power (HP) for an efficiency of 25%. Pearson (1964) and Lefebvre (1964) determined the

---

<sup>5</sup>A complete table with the direct (stroke angle, angle of asymmetry, flight speed) and derived (relative downstroke time, angular velocity, velocity ratio, time factor) parameters, the two factors  $z$  and  $k$ , and the resulting powers is available from the authors upon request.

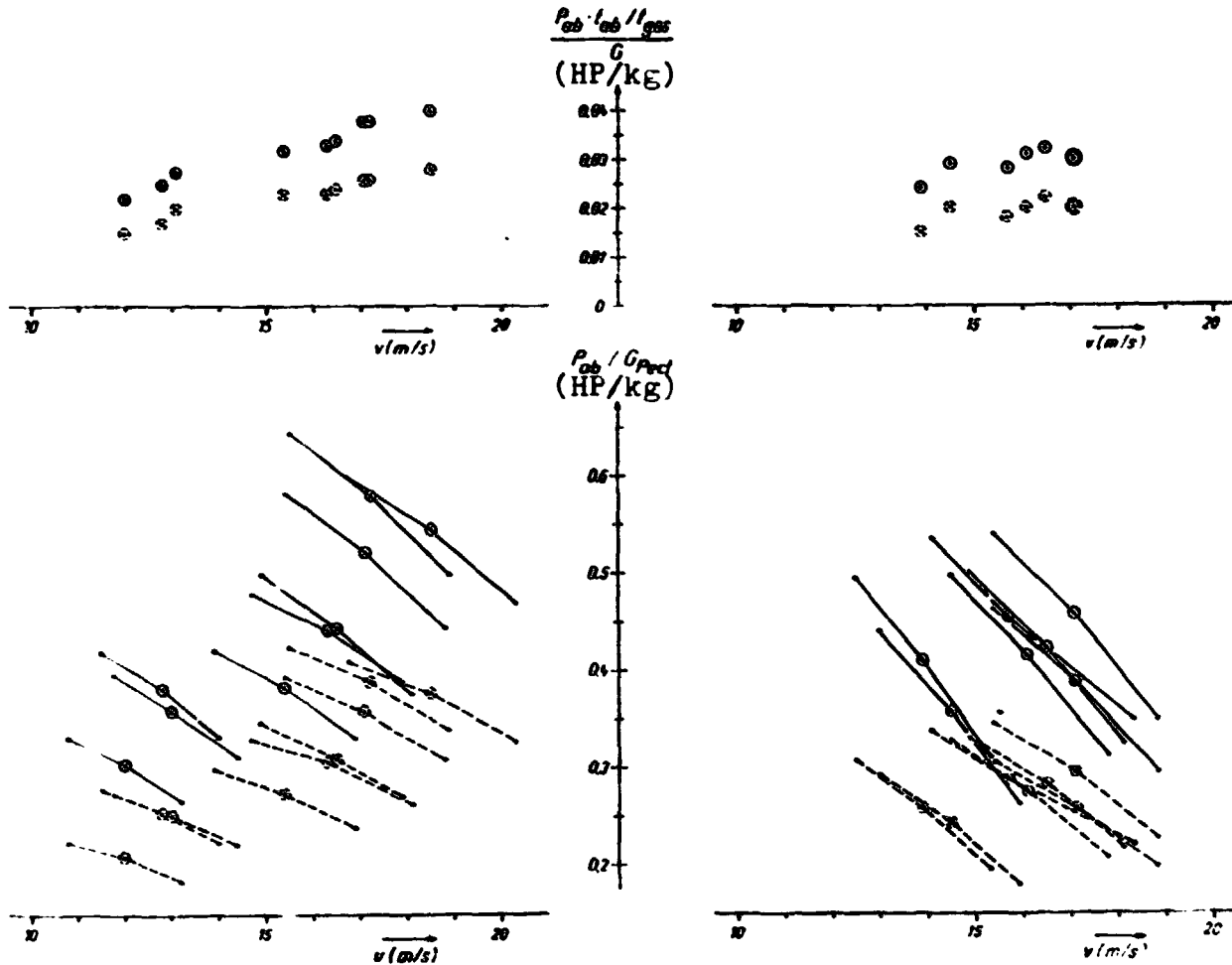


Fig. 12. Specific power of the pectoral muscles (bottom) and the downstroke power (top) converted to the entire stroke cycle of nine pigeons (left) and seven Turkish doves (right). Solid lines: Calculations with  $\bar{H}_{auf} = 0.5\bar{H}_{ab}$ ; broken lines: calculations with  $\bar{H}_{auf} = \bar{H}_{ab}$ . Circles designate average values.

total energy consumption of flying pigeons. If energy production at rest (standard metabolic rate, resting metabolic rate) is known the average energy requirement of the pectorals in flight is equal to the total energy consumption minus the resting metabolic rate and minus the increased power consumption

of muscles other than the pectorals (wing-lifting muscles, heart, respiratory musculature, etc.). The increased power consumption due to muscles other than the pectorals was assumed to be three times as great as the resting metabolic rate. This is based on the following highly simplified derivation. Zeuthen (1942) found the power consumption of flying pigeons to be between and 10 and 27 times the resting metabolic rate, Pearson (1964) found it to be 23 times the latter, and Lefebvre (1954) 10 times the resting metabolic rate. We will use a figure of 18 times the resting metabolic rate and estimate the power consumption during flight of organs not directly participating in the work of flight to be twice the resting metabolic rate. The remaining 16 times the resting metabolic rate must be divided between the pectorals and the other flight muscles. For the latter, we substitute the most important wing-lifting muscle, the *M. supracoracoideus*. In the pigeon, this muscle /452 weighs about 1/7 as much as the pectoral. Assuming the same average metabolic intensity in both muscles, we assign 14 times the resting metabolic rate to the two pectorals and twice the resting metabolic rate to the wing-lifting muscles. Therefore, the average power consumption of the pectorals is equal to the total power consumption minus four times the resting metabolic rate. The amount subtracted may be too large, but it is a safeguard against finding too large a caloric equivalent as a confirmation of mechanical powers which are too large. We emphasize once more that this scheme serves only for estimating the order of magnitude, since it is more likely that the *supracoracoideus* does not have the same rate of power consumption (cf. George and Berger 1966) and is active only in the first part of the upstroke, in which the inner part of the wing is raised into position for the next downstroke, and the adductors bend the pinion joint, while the pectoral must already perform holding work, while the abductors bring the pinion into the starting position for the next downstroke (cf. Oehme 1968b).

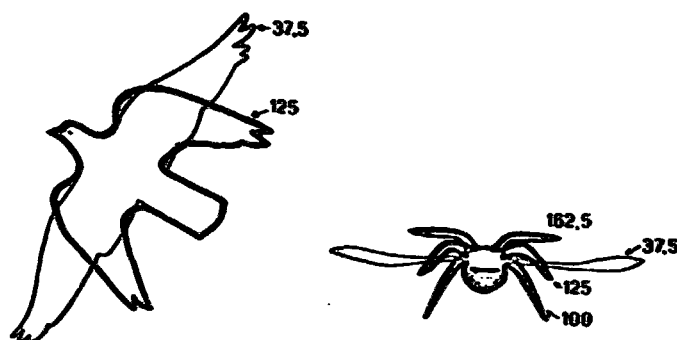


Fig. 13. Wing position and wing area in downstroke and upstroke of *Columbia livia* (left, view from below) and *Streptopelia decaocto* (right, view from rear). Derived from superimposed time-lens photographs, the numbers are the time in msec from start of downstroke.

TABLE V. POWER CONSUMPTION AND AVERAGE RELATIVE PECTORAL POWER OF *COLUMBIA LIVIA*

	Tot. power cons. (TPC) kcal/kg/h	Rest. met. rate (RMR) kcal/kg/h	TPC-4RMR kcal/kg/h	$(\bar{P}_{ab} \cdot t_{ab} / t_{tot}) \cdot 4$ HP/kg
(a)	112 (max at	4.3 (c)	94.8	0.038
	13 m/s < v < 14 m/s)	5.25 (d)	91	0.036
		7 (b)	84	0.033
	84 (75% of max at	4.3	66.8	0.026
	13 m/s < v < 14 m/s)	5.25	63	0.025
		7	56	0.022
(b)	71.8 (max at	4.3	54.6	0.022
	v <sub>s</sub> = 17.9 m/s)	5.25	50.8	0.020
		7	43.8	0.017
	58 (av. at	4.3	40.8	0.016
	11.2 m/s < v <sub>s</sub> < 18.8 m/s)	5.25	37	0.015
		7	30	0.012

In Table 5, the results for 4 different total energy consumption figures are listed with three different resting metabolic rates in each case. The latter also differ by quite a bit. The values derived from the findings of Pearson agree well with those for

$\bar{H}_{auf} = 0.5\bar{H}_{ab}$  (Fig. 12), if one starts from a smaller total value and correspondingly smaller speeds, and even the rate of 112 kcal/kg/h given as an upper bound by Pearson leads to satisfactory agreement with the relative downstroke powers calculated for moderate and high speeds. However, they conflict conspicuously with Lefebvre's findings. For his upper bound, there are, when the velocity is ignored, just barely some correspondences under the assumption that  $\bar{H}_{auf} = \bar{H}_{ab}$ . For his average value, on the other hand, there is no longer any agreement for this case, even if the powers which are about 7% lower with a different coefficient distribution (3) are used. In order to obtain such low values of  $(\bar{P}_{ab} \cdot t_{ab}/t_{ger})/G$ , one would have to make the unrealistic hypothesis that  $\bar{H}_{auf} > \bar{H}_{ab}$ . A number of objections to Lefebvre's analyses must not be ignored. Determination of energy consumption by means of  $CO_2$  /453 production with aid of isotopically labelled water ( $D_2O$ ,  $H_2O^{18}$ ) yields satisfactory results with laboratory monitoring of the experimental animals. This constant observation was not present as the doves in the experiment made the roughly 500 km overland flight. For some birds, interruption of the flight, and food and water intake were conceded. However, this cannot be ruled out for all the birds analyzed. The velocity over the ground ( $v_g$ ) was deduced from the time between departure and arrival and the distance between start and destination. No information on wind conditions was provided for the many hours of flight. It is not at all difficult to acquire a much higher energy consumption rate (relative to pure flight time) by assuming just a moderate head wind and allowing the birds pauses on the ground for roughly 1 hour. The conjecture that undetected influences affected the experimental animals is strengthened by some of the data reported: when two birds fly at almost the same "speed" but the specific energy consumption rate of one is about 1.8 times as great as that of the other, or when the specific energy consumption rates of

two birds are the same, but the "speeds" differ by a factor of 1.7, this can hardly be explained as random fluctuation. For these reasons, Lefebvre's results are not considered evidence against the computing method employed. This view can be supported by other findings. Tucker (1968a, b; 1969), in studies on parakeets (*Melopsittacus undulatus*) and gulls (*Larus atricilla*) flying in a wind tunnel, determined energy consumption rates which make the magnitudes of our calculated results quite believable (see Table 6). In calculating  $(\bar{P}_{ab} \cdot t_{ab}/t_{ges})/G$ , only three times the resting metabolic rate was subtracted from the total consumption, because the supracoracoideus weighed only 1/10-1/12 as much as the pectoral. The values at comparable speeds were distinctly higher for the parakeet than for the pigeon. Probably it generates less /454 lift in the upstroke ( $\bar{H}_{auf} < 0.5\bar{H}_{ab}$ ). Since no data on the flight motion is available, we cannot make even an estimate. However, the size of the converted relative downstroke power speaks for itself and even suggests that the total rate of 112 kcal/kg/h, which Pearson considered an upper bound for the pigeon, may be normal at that speed. The calculated values would be clearly too small, unless  $\bar{H}_{auf} = 0.5\bar{H}_{ab}$ . For the gull, the values are low as compared with those for the pigeon. An estimate with very approximate parameters for the comparable-sized lake gull (*Larus ridibundus*) leads to good agreement. For two flights, with

$$t_{ab}/t_{ges} \approx 0.35(0.35), \quad \varphi_0 - \varphi_u \approx 70^\circ(70^\circ), \quad \delta \approx 0^\circ(1^\circ), \\ n \approx 2(3), \quad v \approx 9 \text{ m/s}(13 \text{ m/s}), \quad \bar{\omega} \approx 8/\text{s}(11.7/\text{s}), \quad \bar{\lambda} \approx 2.4(2.4),$$

$R \approx 0.46 \text{ m}$  and  $G \approx 0.3 \text{ kg}$ , the results were  $(\bar{P}_{ab} \cdot t_{ab}/t_{ges})/G = 0.013 \text{ HP/kg}$  ( $0.018 \text{ HP/kg}$ ) for  $\bar{H}_{auf} = 0.5\bar{H}_{ab}$  and  $0.009 \text{ HP/kg}$  ( $0.012 \text{ HP/kg}$ ) for  $\bar{H}_{auf} = \bar{H}_{ab}$ . The possibility  $\bar{H}_{auf} > 0.5\bar{H}_{ab}$  can be entirely eliminated. It can therefore be concluded that the assumption  $\bar{H}_{auf} = 0.5\bar{H}_{ab}$  is consistent with actual conditions

for the medium-sized birds dealt with here, and that the assumption made in deriving the procedure that the coefficients remain constant is nearly correct.

TABLE VI. POWER CONSUMPTION AND AVERAGE RELATIVE PECTORAL POWER (according to Tucker 1968a, b; 1969)

	Tot. power cons. (TPC) kcal/kg/h	Rest. met. rate (RMR) kcal/kg/h	TPC - 3RMR kcal/kg/h	$(\bar{P}_{ab} \cdot t_{ab}/t_{ges})/G$ HP/kg
<i>Melo- psittacus undulatus</i>	105 (v = 9.7 m/s)	8.2	80.4	0.032
	122 (v = 11.7 m/s)	8.2	97.4	0.039
	161 (v = 12.8 m/s)	8.2	136.4	0.054
	50 (min at 8.5 m/s < v < 12.5 m/s)	4.4	36.8	0.015
<i>Larus atricilla</i>	60 (max at 8.5 m/s < v < 12.5 m/s)	4.4	46.8	0.019

Returning to the original subject of the investigation, it can now be considered certain that the specific power output of the pectoral muscles of the two species of dove under continuous rhythmic load is 10 to 20 times the specific output of mammalian muscles. This does not include the chiroptera, because aerodynamic features similar to those of powered avian flight suggest that the output of the musculature is correspondingly high. Specific muscular output between 0.26 and 0.60 HP/kg -- that is 190 W/kg to 440 W/kg, which after a conversion with  $n = 0.25$ , about 660 kcal/kg/h to 1500 kcal/kg/h -- must be reflected in physiological and morphological features of this high-power muscle. George and Berger (1966) explain what makes this unique vertebrate muscle capable of such high metabolic and energy-utilization rates: a rich supply of blood /455 vessels, extraordinary development of the enzyme apparatus necessary for respiratory-chain phosphorylation, and the burning of fat as the most energy-rich nutrient, another factor being that in the pigeon -- and presumably for the Turkish dove as well -- the entire muscle is not in action during continuous

exertion, but only the red muscle fibers (which are, more numerous), while the less numerous white fibers can supply transient power peaks. Lately, doubts have been expressed regarding this view (Lee 1971), and it is therefore a good idea to devote renewed attention to the relationships between mechanical power and cytophysiological and cytomorphological features. For one side of the problem, the determination of high power, the method presented here will be quite useful when applied to other species, and can be made even more informative by refining the measuring techniques or allowing for the mass of the wing (calculating the moment of inertia). Another thing which should be checked is whether a particular species might be better represented in comprehensive series of measurements by a "standardized" individual with the parameters of the averages and their average errors. Also worth investigating is the relationship between energy utilization rate and flight speed found by Tucker (1968a, b) for the parakeet. This cannot yet be done with the results presented here, because velocity was not determined accurately enough, although a higher speed = higher power trend can be recognized. However, the material is not adequate to fix an upper limit on power and to establish a velocity range for most efficient flying. It would not be possible to obtain Tucker's typical U-shaped curve for energy utilization rate vs. speed over the whole range, because low speeds give rise to different aerodynamic conditions (braked flight, hovering), for which the numerical method employed here cannot be used.

Lastly, we should also mention some other attempts at solving the problem of the flight power of birds from the physical-aerodynamic angle. Although earlier works (Oehme 1963, 1965, 1968a) did start with the basic concept of the propeller model, they then attempted a highly detailed execution with the required parameters, which could only be assumed throughout.



Moreover, a calculating method from propeller engineering was used to obtain an effective radius of  $0.7 R$ , without making adequate allowance for the wing geometry of birds. Consequently, the powers obtained at that time were too large and were revised in conjunction with the application of the new methods. Pennycuick (1968b), in his studies on energy expenditure by pigeons in horizontal flight, took a somewhat different theoretical approach. Since his findings led him to more general conclusions on flight power (Pennycuick 1969), this work must be discussed in somewhat more detail. He derived total flight power from three components: the weight of the bird, the profile drag of the wing, and the body drag. Doubts can be legitimately be raised regarding the usability of the coefficients employed for the aerodynamic forces. These coefficients were obtained /456 from wind-tunnel studies (Pennycuick 1968a), which in no way reproduced normal gliding flight, but instead corresponded more or less closely to a landing approach with strong deceleration (see also Oehme 1970a). Also, the doves used in the flight studies obviously could not be made to fly normally, as can be seen from the pictures and descriptions, but instead flew more or less in a "braking attitude" (see Brown 1948; Oehme 1968b). That they were at their power limits at a velocity of 16 m/sec in this arrangement is evident, but to conclude that "the pigeon" is incapable of flying faster over a long period of time is certainly incorrect. If the drag coefficients employed, and the power components calculated from them, were too high, the weight-compensating "induced power" is too small, because the calculations were carried out simply with the induced vertical velocity, ignoring the fact that the wings are making a rotary movement. Moreover, the time course of the wing stroke was rather brutally simplified. Since the errors largely cancel out, the resulting values fit into the spectrum presented here. The long-term power of the 0.4 kg dove is stated to be 8.7 W at  $v = 8$  m/sec and 10.5 W at

16 m/sec. This corresponds to an average relative power ( $\bar{P}_{ab} \cdot t_{ab}/t_{ges}$ )/G of 0.030 HP/kg - 0.036 HP/kg. Pennycuick's idea of handling design questions of flying animals (aerodynamic quality, speed range, optimum traveling speed, range in prolonged flight; their interrelationships and relation to size of animal, etc.) is completely correct. However, a sufficient amount of meaningful data would have assisted the generalization. The method described here will contribute to supplying this data.

### Summary

In order to determine the power of a bird's pectoral muscles in free level flight, a procedure was developed on the basis of an airscrew calculation. The procedure avoids the use of aerodynamic force coefficients, which cannot be measured in the flying bird.

Together with angular velocity, the tangential force necessary to generate the required lift in the downstroke and the distance along the wing from the shoulder joint to the point of application of the tangential force yield the downstroke power.

Required morphological data are the total weight, the weight of the two pectoral muscles, the length of the wing extended in downstroke position, from shoulder joint to wing tip, and the location of the body contour along the wing length.

Kinematic data are obtained from time-lens films. These data are: the duration of the downstroke, the duration of accelerated rotation at the beginning of the downstroke, and the duration of the entire stroke cycle, the flight speed, the stroke angles, and the positions of their angle bisectors relative to the horizontal.

Nine pigeon flights and seven Turkish dove flights are analyzed with the method of calculation. Comparisons with metabolic-physiological studies confirm the usability of this method and also support the theoretical assumptions.

The specific power capacity of the pectoral muscles in both species (0.26-0.60 HP/kg) under prolonged load is 10 to 20 times that of mammal muscles, except, probably, for the flight muscles of bats.

## REFERENCES

1. Bilo, D., "Biophysics of flight of small birds. I. Kinematics and aerodynamics of wing downstroke of house sparrow (*Passer domesticus*)," Z. vergl. Physiol. 71, 382-454 (1971).
2. Brody, S., "Bioenergetics and growth," New York, 1945.
3. Brown, R. H. J., "The flight of birds. The flapping cycles of the pigeon," J. Exp. Biol. 25, (1948), 322-333.
4. "Flight." In: Biology and comparative physiology of birds, Vol. 2, (Ed. A. J. Marshall), New York and London, 1961a.
5. "The power requirements of birds in flight," Symp. Zool. Soc. London No. 5. (1961b), 95-99.
6. Dickinson, S., "The dynamics of bicycle pedalling," Proc. Roy. Soc. London, Ser. B, 103, (1928), 225-233.
7. George, J. C., and A. J. Berger, "Avian myology," New York and London, 1966.
8. Glauert, H., "Airplane propellers." In: Aerodynamic theory, Vol. 6, Div. L, (Ed. W. F. Durand), Berlin, 1935.
9. Henderson, Y., and H. G. Haggard, "The maximum of human power and its fuel," Amer. J. Physiol. 72, (1925), 264-282.
10. Holst, E. von, "On 'artificial birds' as a means for studying avian flight," J. Orn. 91, (1943), 406-447.
11. -- and Kuchemann, D., "Biological and aerodynamic problems of animal flight," Naturw. 29, (1941), 348-362
12. King, J. R., and D. S. Farner, "Energy metabolism, thermo-regulation and body temperature." In: Biology and comparative physiology of birds, Vol. 2, (Ed. A. J. Marshall), New York and London 1961.
13. Lasiewski, R. C., "Oxygen consumption of torpid, resting, active and flying hummingbirds," Physiol. Zool. 36, (1963), 122-140.
14. -- and Dawson, W. R., "A re-examination of the relation between standard metabolic rate and body weight in birds," Condor 69, (1967), 13-23.
15. Lee, S. Y., "A histochemical study of twitch and tonus fibers," J. Morph. 133, (1971), 253-272.

16. Lefebvre, E. A., "The use of  $D_2O^{18}$  for measuring energy metabolism in *Columba livia* at rest and in flight," Aukj 71, (1964), 403-416.
17. Nachtigall, W., "Glaserne Schwingen," [Glass quills], Munich, 1968.
18. Oehme, H., "Flight and wings of starlings and blackbirds," Biol. Zbl. 82, (1963), 413-454, 569, 587.
19. "Powered flight of large birds," Beitr. Vogelk. 11, (1965), 1-31.
20. "Flight of the swift (*Apus apus*)," Biol. Zbl. 87, (1968a), 287-311.
21. "Powered flight of birds," Vogelwelt 89, (1968b), 20-42.
22. "Wing profiles of starlings and doves," forma et functio 2, (1970a), 266-287.
23. "The hovering of the redstart (*Phoenicurus phoenicurus*)," Beitr. Vogelk. 15, (1970b), 417-433.
24. "The geometric twisting of the avian wing," Biol. Zbl. 90, (1971), 145-156.
25. "The kinematics of the wing stroke in unaccelerated horizontal flight (studies on biophysics and physiology of avian flight I)," Zool. Jb. Physiol. 78, (1974), 461-512).
26. "Geometry of the avian wing (studies on biophysics and physiology of avian flight II)," Zool. Jb. Physiol. 79, (1975), 402-424.
27. Pearson, O. P., "The metabolism of hummingbirds," Condor 52, (1950), 145-152.
28. "The metabolism of hummingbirds," Scientific American 188, (1953), 69-73.
29. "Metabolism and heat loss during flight in pigeons," Condor 66, (1964), 182-185.
30. Pennycuik, C. J., "A wind-tunnel study of gliding flight in the pigeon *Columba livia*," J. Exp. Biol. 49, (1968a), 509-526.
31. "Power requirements for horizontal flight in the pigeon *Columba livia*," J. Exp. Biol. 49, (1968b), 527-535.

32. Pennycuik, C. A., "The mechanics of bird migration," Ibis 111, (1969), 525-556. /458
33. Tucker, V. A., "Respiratory exchange and evaporative water loss in the flying budgerigar," J. Exp. Biol. 48, (1969a), 67-87.
34. "Upon the wings of the wind," New Scientist, June, 1968. (1968b), 694-696.
35. "The energetics of bird flight," Scientific American 220, (1969), 70-78.
36. Zeuthen, E., "The ventilation of the respiratory tract in birds," Kge. Danske Videnskab. Selskab. Biol. Medd. 17, (1942), 1-51.